JTTEE5 17:395–403
DOI: 10.1007/s11666-008-9189-x
1059-9630/$19.00 © ASM International

Microstructure and Properties of HVOF-Sprayed WC-$(W,Cr)_2C$-Ni Coatings

Lutz-Michael Berger, Sabine Saaro, Tobias Naumann, Michaela Kašparova, and František Zahálka

(Submitted October 2, 2007; in revised form February 25, 2008)

The composition WC-$(W,Cr)_2C$-Ni is one of the standard compositions used for the preparation of thermally sprayed coatings by high velocity oxy-fuel (HVOF) spraying. Surprisingly, this composition has been poorly investigated in the past. Frequent use of commercial designations WC-'CrC'-Ni, WC-Cr_3C_2-Ni, and WC-NiCr indicates the insufficient knowledge about the phase compositions of these powders and coatings. The properties of these coatings differ significantly from those of WC-Co and WC-CoCr coatings. In this paper, the results of different series of experiments conducted on HVOF-sprayed WC-$(W,Cr)_2C$-Ni coatings are compiled and their specific benefits pointed out. The focus of this study is on the analysis of the microstructures and phase compositions of the feedstock powders and coatings. Unlike WC-Co and Cr_3C_2-NiCr, WC-$(W,Cr)_2C$-Ni is not a simple binary hard phase—binder metal composite. The phase $(W,Cr)_2C$ with unknown physical and mechanical properties appears as a second hard phase, which is inhomogeneously distributed in the feedstock powders and coatings. As examples of coating properties, the oxidation resistance and dry sliding wear properties are compared with those of WC-10%Co-4%Cr coatings.

Keywords dry sliding wear resistance, HVOF hardmetal coatings, oxidation resistance, WC-CoCr, WC-$(W,Cr)_2C$-Ni

1. Introduction

Feedstock powders and coatings made of the commercially available composition WC-$(W,Cr)_2C$-Ni are based on an invention for which a patent application was filed in 1958 (Ref 1). As opposed to studies on WC-Co and WC-CoCr coatings, studies on these coatings are rarely found in the literature and most of them were performed in Japan. Okada and Yamada investigated the effect of an additional heat treatment on the coating properties (Ref 2). Ishikawa et al. (Ref 3-5) studied the influence of a gas shroud during HVOF-spraying on the microstructure, phase composition, corrosion, and wear properties of the coatings. Nakajima et al. investigated the rolling contact fatigue of HVOF-sprayed coatings (Ref 6-8). The composition was also selected in a number of comparative studies of different hardmetal coatings, e.g., by Toma et al. (Ref 9), Henke et al. (Ref 10), Cho et al. (Ref 11), and Kreye (Ref 12).

The phase composition of the coating in the patent (Ref 1) is given as tungsten monocarbide (WC), a mixed carbide $(W_xCr_y)C_z$, and nickel. In the comparative study published by Kreye (Ref 12), the phase composition WC-25$(WCr)_2C$-5Ni is given. However, nowadays there are confusing designations used in the literature for this one and the same composition, e.g., WC-'CrC'-Ni (Ref 11), WC-Cr-Ni (Ref 6-8), WC-NiCr (Ref 2), and WC-Cr_3C_2-Ni (Ref 9). A phase 'CrC' with a chromium-to-carbon atomic ratio of 1:1 does not exist in the Cr-C phase diagram. As shown below, although Cr_3C_2 sometimes appears in the powders, it is not detected in the coatings. The lack of a JCPDS standard card for the $(W,Cr)_2C$ phase is one of the probable reasons for the contradictory and confusing designations used for this coating composition. The $(W,Cr)_2C$ phase has been described in the literature (Ref 13, 14). Stecher et al. (Ref 13) found a linear decrease in the lattice parameters *a* and *c* with increasing 'Cr_2C' content, as shown in Fig. 1. However, no data on the physical and mechanical properties with varying chromium content are available.

The WC-$(W,Cr)_2C$-Ni coatings are characterized by extraordinary properties. Our investigations showed a much superior oxidation resistance to that of other commercial WC-based coatings (Ref 15). Good corrosion resistance is another important property of this composition (Ref 16), although microcracks can accelerate attack by corrosive solutions (Ref 11). Therefore, the composition WC-$(W,Cr)_2C$-Ni can bridge the gap between WC-Co and Cr_3C_2-NiCr with regard to oxidation and corrosion resistance (Ref 17). The coating shows excellent dry sliding wear properties at 800 °C. At this temperature other WC-based coatings cannot be applied at all (Ref 18).

In this paper the results of different experimental series conducted on HVOF-sprayed WC-$(W,Cr)_2C$-Ni coatings are compiled and their specific benefits pointed out. The focus of this study is on the analysis of the microstructures and phase compositions of feedstock powders produced by

Lutz-Michael Berger, Sabine Saaro and **Tobias Naumann**, Fraunhofer Institute for Material and Beam Technology (Fh-IWS), Dresden, Germany; and **Michaela Kašparova** and **František Zahálka**, Škoda Výzkum s.r.o., Plzen, Czech Republic. Contact e-mail: sabine.saaro@iws.fraunhofer.de.

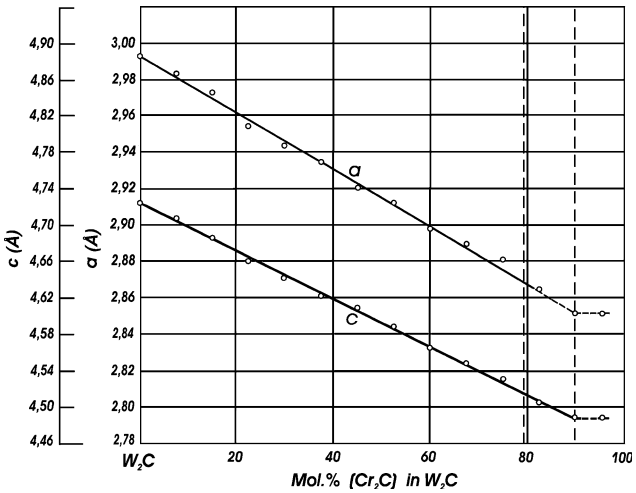

Fig. 1 Changes in lattice parameters *a* and *c* as a function of chromium content in W_2C after Stecher [13]

various techniques and coatings sprayed using different HVOF systems. As examples of coating properties, the oxidation resistance and dry sliding wear properties are compared with those of WC-10%Co-4%Cr coatings. The real phase composition WC-$(W,Cr)_2C$-Ni is used throughout this paper for the designation of all powders and coatings.

2. Experimental

Commercial WC-$(W,Cr)_2C$-Ni feedstock powders prepared by agglomeration & sintering (a & s) and sintering & crushing (s & c) were used in all experimental series described below. The particle size distributions of the feedstock powders were selected according to the requirements of the HVOF systems used. In all cases the coatings were deposited on to grit-blasted substrate surfaces with optimized parameter sets. Spraying was performed with four different HVOF systems: JP-5000 (Praxair, USA), K2 (GTV mbH, Germany), DJH 2700 (SulzerMetco AG, Switzerland), and TopGun (UTP, Germany).

From the feedstock powder characteristics studied, the cross sections investigated by scanning electron microscopy (SEM) and the phase compositions investigated by X-ray diffraction (XRD) are the focuses of this paper.

Detailed studies on the influence of the feedstock powder on coating microstructure and phase composition were performed with coatings sprayed by kerosene-fuelled JP-5000 and K2 systems. In these cases coatings were sprayed on to mild steel substrates of dimension 60 × 100 mm. From the results obtained, the phase compositions and microstructures obtained from the metallographic cross-sections studied by SEM and the hardness values are highlighted in this paper.

In the oxidation experiments, coatings sprayed by ethene-fuelled DJH 2700 and TopGun systems from an a & s powder with optimized spray parameter sets were used. The coatings were deposited onto a 45 × 20 mm surface of a 6 mm thick oxidation-resistant steel substrate (1.4021, X20Cr13). The oxidation experiments were performed in a tube furnace in streaming air with a flow rate of 10 l/h. The heating rate was 2 K/min. The experiments were carried out using different combinations of temperature (350-900 °C) and time (2-128 h). More detailed information on these experiments are given in a paper by Berger et al. (Ref 15).

WC-$(W,Cr)_2C$-Ni coatings were also part of a systematic comparative study of HVOF-sprayed hardmetal coatings under dry sliding conditions up to 800 °C (Ref 18-21). These tests were performed at the Federal Institute for Materials Research and Testing (BAM) in Berlin, Germany, according to DIN 50324 (ASTM G-99) with a BAM-designed high-temperature tribometer. Coatings were deposited on one planar surface of the steel (1.3910, Invar, Ni36) test specimen by an ethene-fuelled DJH 2700 system using an a & s feedstock powder. For all coatings, the minimum as-sprayed thickness was approximately 250 μm. Sintered alumina (99.7%) bodies were used as the counterparts. A normal force of 10 N was applied and the sliding distance was 5,000 m. Experiments were performed at 23, 400, 600, and 800 °C in air with sliding speeds of 0.1, 0.3, 1, and 3 m/s.

3. Results and Discussion

3.1 Microstructures and Phase Compositions of Feedstock Powders

Commercial WC-$(W,Cr)_2C$-Ni powders made using various techniques, e.g., agglomeration & sintering (a & s), sintering & crushing (s & c), and agglomeration & plasma densification, are available. Figure 2 shows SEM micrographs of the cross sections of one s & c and two a & s WC-$(W,Cr)_2C$-Ni powders, selected as characteristic examples. The powder particles of the s & c powders are dense, while the particles of the a & s powders are porous. As can be derived from the different grayscales, all powders are characterized by the appearance of at least three phases, which have in part inhomogeneous distributions. The diffraction patterns of these selected powders are illustrated in Fig. 3. WC was identified as the main constituent, and metallic nickel was found to be present in all these powders. Peaks of the $(W,Cr)_2C$ phase could be detected in the diffraction patterns of the s & c powder and one a & s powder (see line b in Fig. 3). This a & s powder also contained alloyed Cr_7C_3, with peaks shifted in comparison to those of the JCPDS standard. The other a & s powder (see line c in Fig. 3) contained Cr_3C_2 as a second carbide phase, but no $(W,Cr)_2C$. No chromium carbides were found in the s & c powder.

EDX mapping provided more insight into the distribution of the phases. As an example, the element maps for tungsten, chromium, and nickel are shown for the s & c powder in Fig. 4. Areas with WC and Ni were found to coexist with large areas consisting of $(W,Cr)_2C$.

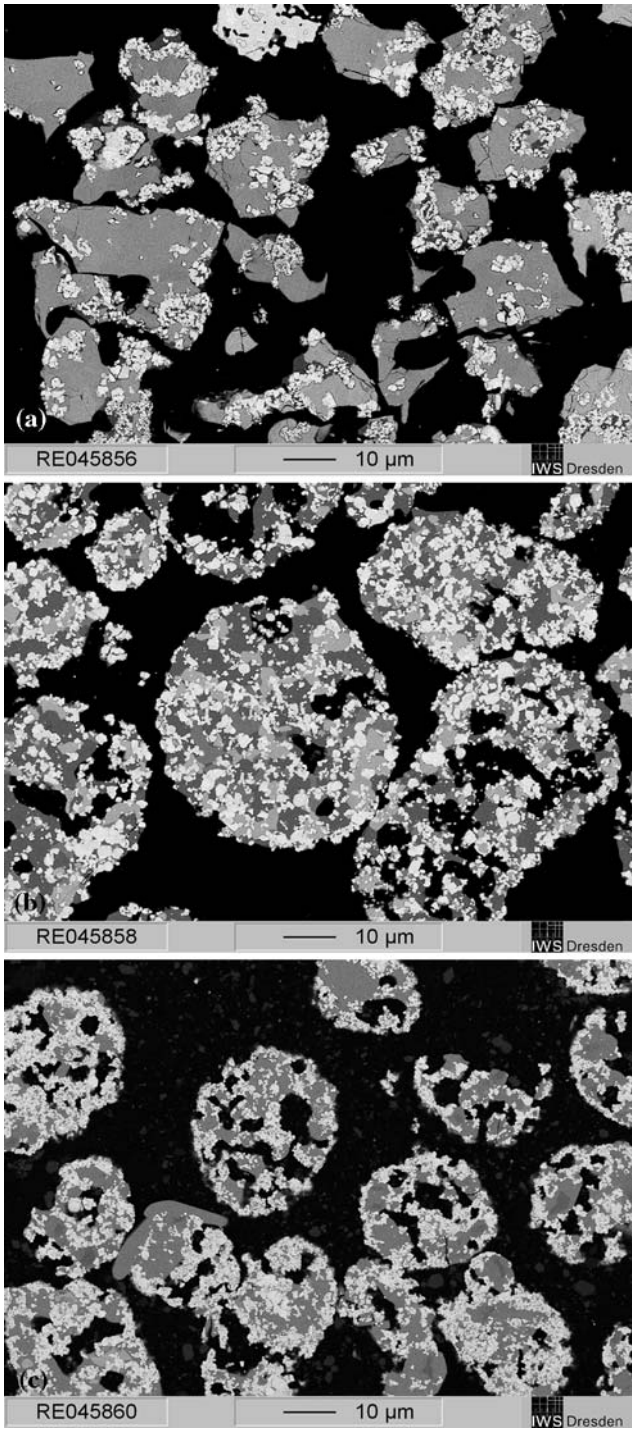

Fig. 2 SEM (BSE) images of feedstock powder cross-sections: (a) sintered & crushed, (b) agglomerated & sintered, producer 1, and (c) agglomerated & sintered, producer 2

Based on the linear dependence of the lattice parameters *a* and *c* on the chromium content (see Fig. 1), it was found that in all powders containing the $(W,Cr)_2C$ phase, the 'Cr_2C' content varied in a wide range of 10-70 mol per cent. The lattice parameters of this phase for the powders shown in Fig. 2 are compiled in Table 1. Due to the

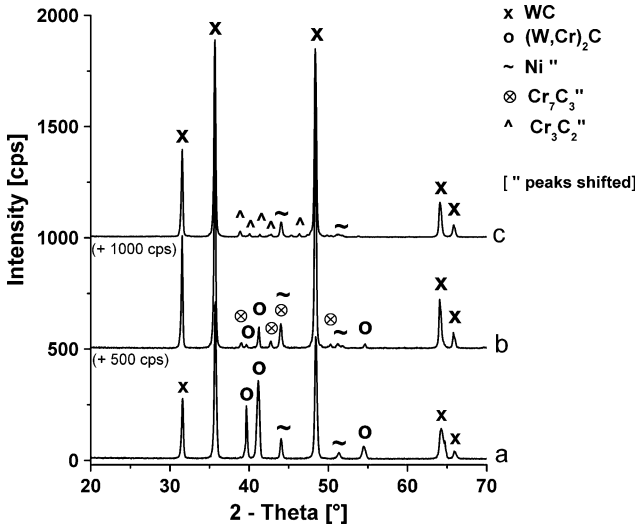

Fig. 3 Diffraction patterns of the WC-$(W,Cr)_2C$-Ni powders: sintered & crushed (line a) and agglomerated & sintered powders from producers 1 (line b) and 2 (line c)

varying tungsten and chromium contents, the grayscale of this phase in relation to the other phases can vary significantly in the SEM micrographs.

One can speculate that fine WC, Cr_3C_2 and Ni powders are the starting materials for feedstock powder preparation. Sintering of the starting materials is accompanied by several metallurgical reactions. As a result of these reactions, Cr_3C_2 is depleted and $(W,Cr)_2C$ is formed. Therefore, the amounts of these two phases in the feedstock powder depend on the completeness of the reactions during sintering. Cr_7C_3 is presumably an intermediate reaction product.

Therefore, WC-$(W,Cr)_2C$-Ni feedstock powders do not represent classic hardmetal composites such as plain WC-Co and Cr_3C_2-NiCr, where one type of hard carbide particles is embedded in a metal binder matrix (Ref 22). Here, at least two hard phases were present as a rule. It is understandable that the behavior and metallurgical processes occurring during spraying of this composition will be totally different from those of plain WC-Co feedstock powders (Ref 23, 24). Currently no conclusions on the dependence of processability and coating properties on feedstock powder phase composition can be made.

3.2 Microstructures, Phase Compositions, and Hardness Levels of As-Sprayed Coatings

The SEM micrographs given in Fig. 5 to illustrate the microstructures of WC-$(W,Cr)_2C$-Ni coatings show two different magnifications of the cross sections of coatings sprayed with a JP-5000 system from the s & c powder (see cross section in Fig. 2a and the XRD pattern in Fig. 3, line a) and the a & s powders (see cross section in Fig. 2c and the XRD pattern in Fig. 3, line c). In general, the microstructures appeared to be even more complex than those which the WC-Co and WC-CoCr coatings are known to have. Bright particles in the micrographs corresponded to WC.

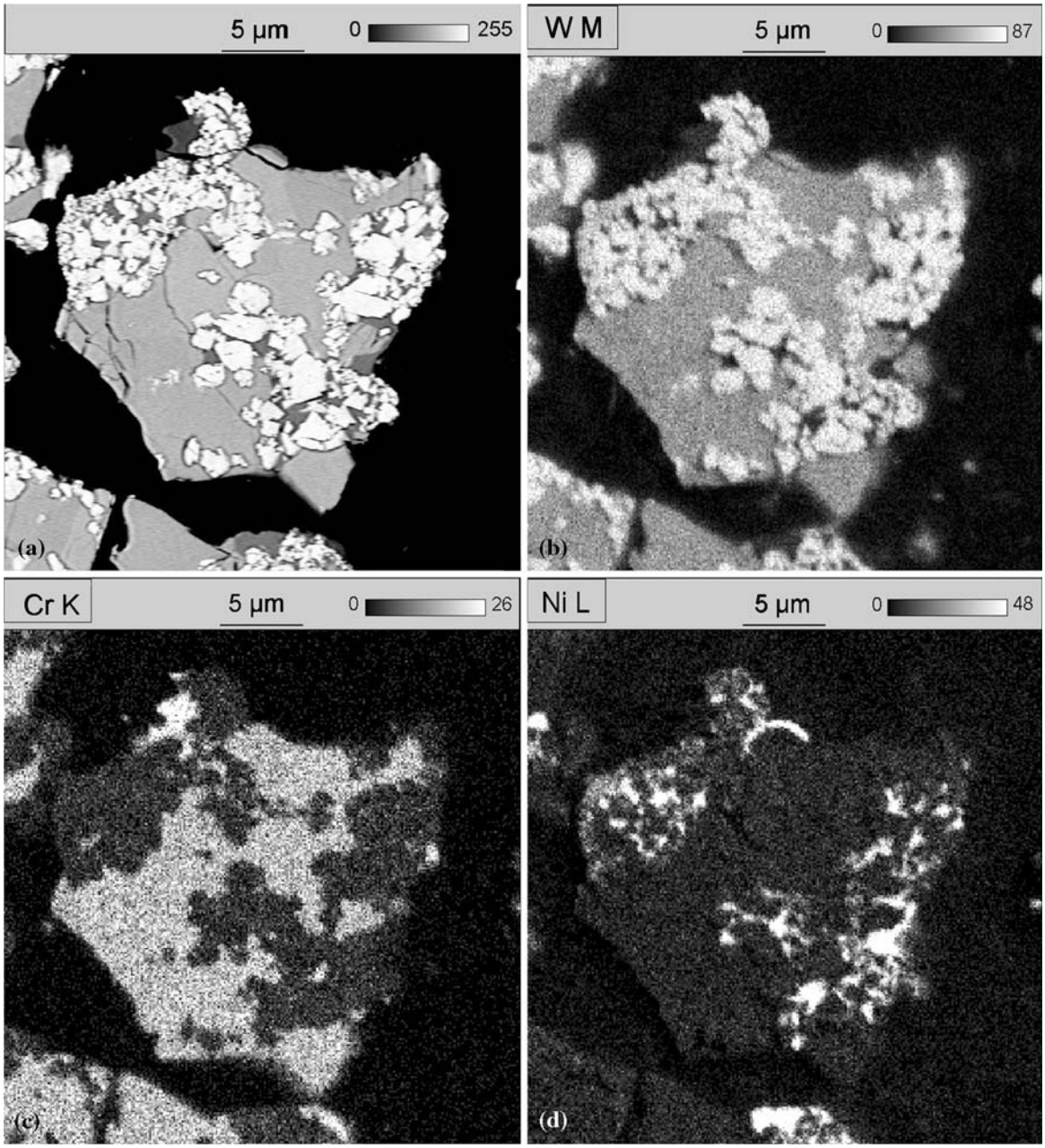

Fig. 4 EDX mappings of the cross section of an s & c powder: (a) BSE image, (b) distribution of tungsten, (c) distribution of chromium, and (d) distribution of nickel

The WC content in the coating prepared from the s & c powder (see Fig. 5a and b) was significantly lower than that in the coating prepared from the a & s powder (see Fig. 5c and d). In addition, the WC particles were more heterogeneously distributed in the coating prepared from the s & c powder. This is in good agreement with the microstructures of the corresponding powders.

The corresponding XRD patterns are given in Fig. 6. The intensities of the different phases correlate well with the information from the SEM micrographs shown

Table 1 Lattice parameters *a* and *c* of the $(W,Cr)_2C$ phase for the feedstock powders and the coatings sprayed by JP-5000 system

Feedstock powder	Lattice parameters of the feedstock powder, nm	Lattice parameters of coating, nm
s & c	$a = 0.289$; $c = 0.454$	$a = 0.290$; $c = 0.459$
a & s, producer 1	$a = 0.288$; $c = 0.454$	$a = 0.288$; $c = 0.452$
a & s, producer 2	...	$a = 0.297$; $c = 0.470$

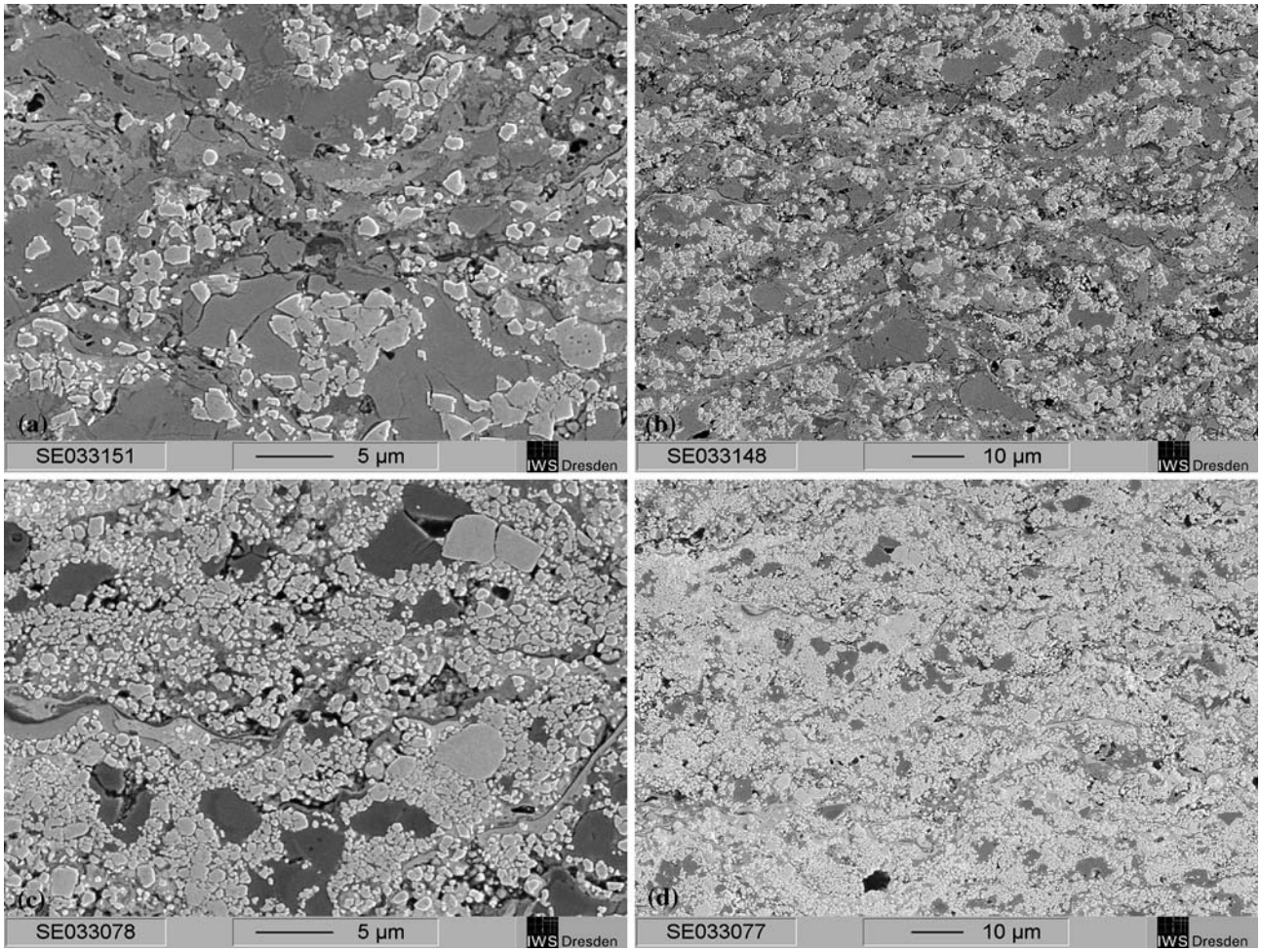

Fig. 5 SEM (SE) images of the cross sections of coatings sprayed by JP-5000: (a) and (b) sintered & crushed powder, (c) and (d) agglomerated & sintered powder

in Fig. 5. The lower WC content in the coating prepared from the s & c powder corresponds well with the higher $(W,Cr)_2C$ content. Furthermore, Cr_2O_3 could be detected in the XRD patterns of this coating, as shown in Fig. 6 (line a).

The lattice parameters of the $(W,Cr)_2C$ phase for the coatings prepared by JP-5000 are also compiled in Table 1. It appears that the chromium content of the $(W,Cr)_2C$ phase was lower in the coatings than in the feedstock for the s & c powder and the a & s powder from producer 1. The phase $(W,Cr)_2C$ was not found in the a & s powder from producer 2, whereas it was found in the coating. This indicates that either the $(W,Cr)_2C$ phase can easily be formed or its tungsten/chromium ratio can change as a result of the spray process.

The oxygen content of WC-$(W,Cr)_2C$-Ni coatings was given as 1.72 mass% (Ref 16), significantly higher than that of the other WC-based hardmetal coatings (0.12% and 0.36% for WC-Co and WC-10Co4Cr, respectively). Ishikawa et al. (Ref 5) found an oxygen content of up to about 1.6 mass%, depending on the spray conditions. This high oxygen uptake can be attributed to the higher chromium content.

Coating hardness is frequently measured. The hardness values for the coatings sprayed with JP-5000 and K2 systems from feedstock powders described in this section varied between 900 and 1150 HV0.3. In the other experimental series discussed below, the coating sprayed from an a & s powder with the DJH 2700 system showed a hardness of 970 HV0.3, while the hardness of a coating sprayed with TopGun was measured to be 1250 HV0.3.

Values in the literature for JP-5000-sprayed coatings (Ref 11) are in the same range as the hardness values (about 1000 HV0.3) found by us, but much higher values (up to 1650 HV0.3) have also been reported (Ref 5). Other HV0.3 hardness values for WC-$(W,Cr)_2C$-Ni coatings reported in the literature (Ref 16, 25) are compiled together with those of other selected WC-based coatings in Table 2. The hardness values give a rather contradictory picture regarding the ranking of the WC-$(W,Cr)_2C$-Ni coatings compared with other WC-based coatings.

3.3 High Temperature Oxidation of the Coatings

Oxidation limits the application of thermally sprayed coatings at high temperatures in air, especially in the case

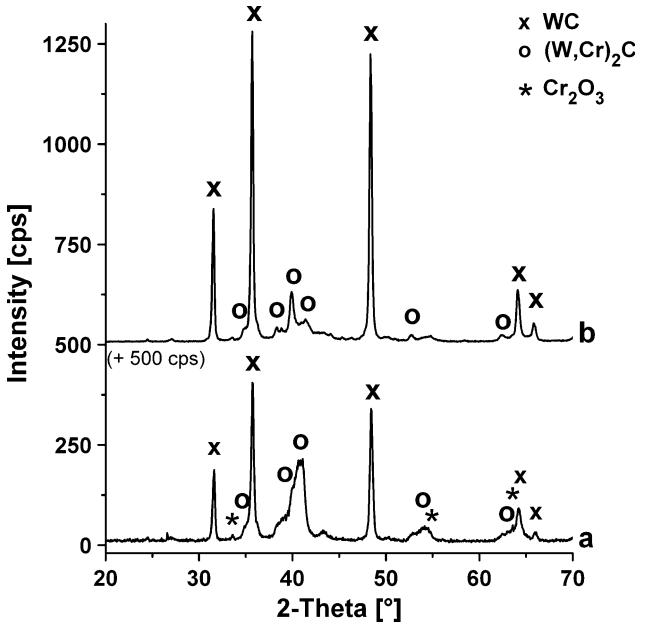

Fig. 6 XRD diffraction patterns of the coatings illustrated in Fig. 5: sintered & crushed powder (line a) and agglomerated & sintered powder from producer 2 (line b)

Table 2 Hardness values (HV0.3) from the literature for selected WC-based coatings

Composition	Data taken from Ref. 16	Data taken from Ref. 25
WC-12%Co	1376 ± 78	1250 ± 50
WC-10%Co4%Cr	1437 ± 90	1350 ± 50
WC-$(W,Cr)_2C$-Ni	1242 ± 68	1300 ± 50

of WC-Co coatings having an application limit of approximately 500 °C. A general increase in the application limit has been expected to be achieved through alloying with chromium (Ref 26), but as shown below, this holds true only for WC-$(W,Cr)_2C$-Ni and not for WC-10Co4Cr. The high oxidation resistance of the WC-$(W,Cr)_2C$-Ni coatings was also confirmed by Ishikawa et al. (Ref 5).

According to SEM micrographs of coating cross sections after oxidation at 700 °C for 2 h in air, the oxide scale thickness was different for the WC-10Co4Cr and WC-$(W,Cr)_2C$-Ni coatings sprayed by TopGun from a & s powders. The thickness of the WC-CoCr coating was approximately 5-10 μm, whereas the oxide scale on the WC-$(W,Cr)_2C$-Ni coating was so thin that it could not be measured. Therefore, it is more appropriate to study the oxide scales by X-ray diffraction, where the patterns are taken from the surface of the coatings. The patterns for the as-sprayed condition and after oxidation at 700 °C for 2 h in air are shown for the WC-CoCr coating in Fig. 7a and for the WC-$(W,Cr)_2C$-Ni coating in Fig. 7b. In the as-sprayed coatings for both compositions, due to the spray conditions with the TopGun process (direct

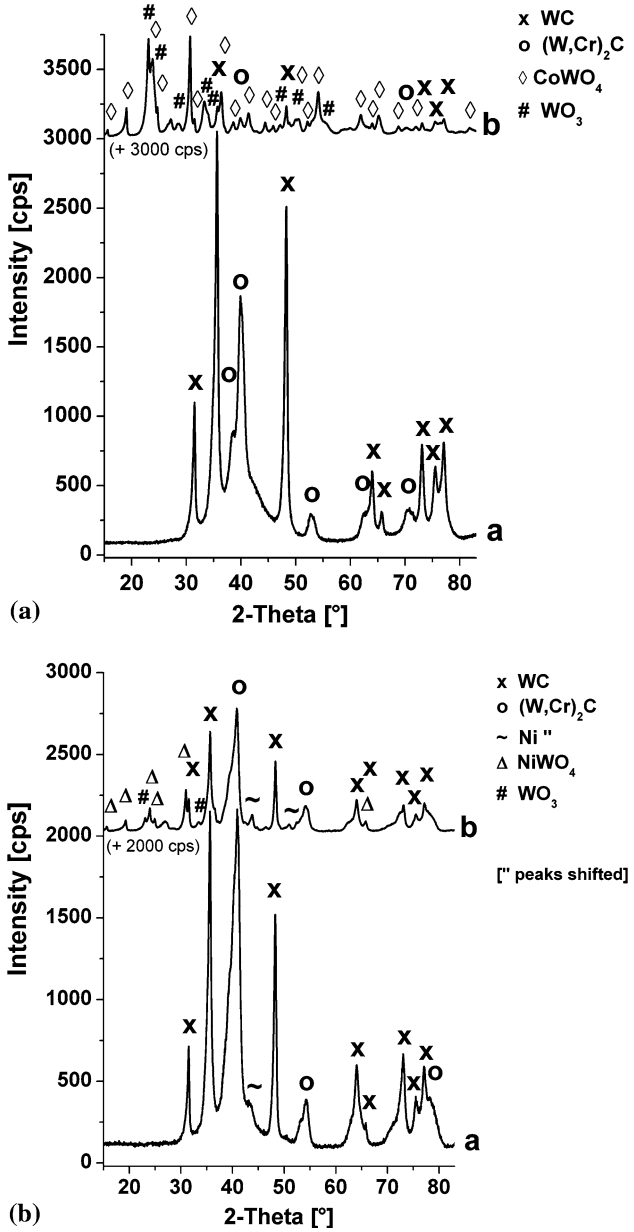

Fig. 7 (a) Diffraction patterns of the as-sprayed (TopGun) WC-CoCr coating (line a) and after oxidation at 700 °C/2 h (line b) (b) Diffraction patterns of the as-sprayed (TopGun) WC-$(W,Cr)_2C$-Ni coating (line a) and after oxidation at 700 °C/2 h (line b)

injection of the feedstock into the combustion chamber), a lower amount of WC and a higher amount of the $(W,Cr)_2C$ phase were observed. After oxidation, the thin oxide scale thickness is responsible for the fact that the phases of the as-sprayed coating (WC, $(W,Cr)_2C$ and Ni) were still detectable in the diffraction pattern. WO_3 and $NiWO_4$ were the detectable constituents of the oxide scale at this temperature. Due to the higher oxide scale thickness of the WC-CoCr coating, only a few small peaks of WC and $(W,Cr)_2C$ were detectable. The oxide scale consisted of WO_3 and $CoWO_4$.

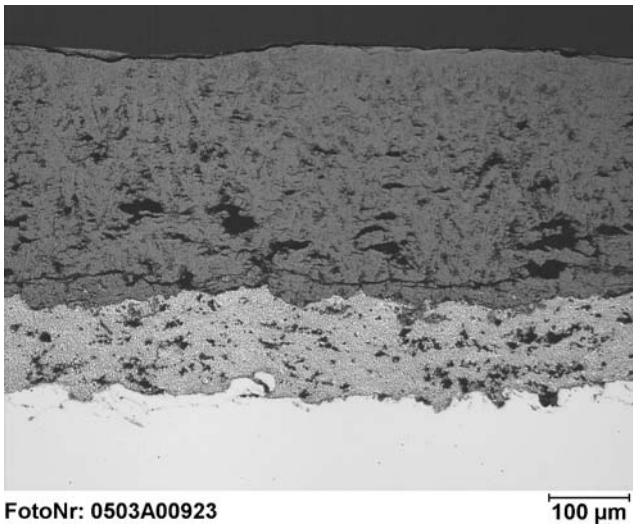

Fig. 8 Optical micrograph of the WC-CoCr coating (thickness of the hardmetal coating about 120 µm) with oxide scale, taken from a tribological specimen after testing at 800 °C and 1 m/s (total oxidation time about 90 min) in the area of the wear track [18]

The differences in oxidation resistance of these two compositions were also demonstrated through microstructural investigation of tribological samples after high-temperature dry sliding testing. Figure 8 shows an optical micrograph of the WC-CoCr coating with the oxide scale formed, taken from a tribological specimen after testing at 800 °C and 1 m/s (total oxidation time about 90 min) in the area of the wear track (Ref 18). The total coating thickness inside the wear track after testing was about 400 µm, higher than the coating thickness after lapping of about 250 µm. The coating and the oxide scale outside the wear track had the same structures, but the oxide scale thickness was about 400 µm. This indicates an increase in the coating volume by oxidation. In contrast, Fig. 9 shows an SEM micrograph of the near-surface region of the WC-$(W,Cr)_2C$-Ni coating outside the wear track after wear testing at 800 °C and 0.1 m/s (total oxidation time about 14 h) (Ref 18). This micrograph again indicates that evidence of the very thin oxide scale is difficult to provide by metallographic preparation.

3.4 Tribological Studies

In this section, a few selected results for the WC-$(W,Cr)_2C$-Ni and WC-10Co-4Cr coatings from a comparative study of HVOF-sprayed hardmetal coatings paired with sintered alumina for high-temperature dry sliding experiments (Ref 18-21) are illustrated in Fig. 10 (total volumetric wear coefficient) and Fig. 11 (coefficient of friction). Under the test conditions, the wear of the sintered Al_2O_3 counterparts was negligible compared with that of the coatings. Results for self-mated pairs are described elsewhere (Ref 18, 27).

For all temperatures, the total wear coefficients of WC-$(W,Cr)_2C$-Ni coatings, illustrated in Fig. 10, were nearly independent of sliding speed. Including the results

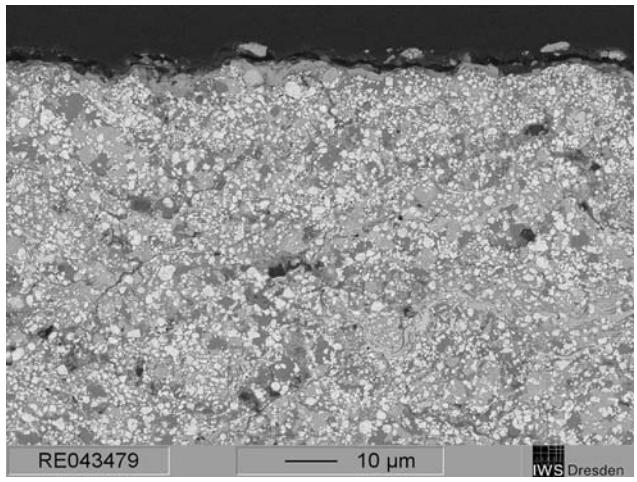

Fig. 9 SEM micrograph (BSE mode) of a WC-$(W,Cr)_2C$-Ni coating outside the wear track after wear testing at 800 °C and 0.1 m/s (total oxidation time about 14 h) [18]

obtained at the highest test temperature of 800 °C, the total wear coefficients were about 10^{-6} mm^3/Nm. The total wear coefficients of WC-10Co-4Cr were found to be below 10^{-6} mm^3/Nm for most of the sliding speeds at room temperature and at 400 °C. At 600 °C, the total wear rate for WC-10Co-4Cr was about 10^{-6} mm^3/Nm. The total wear coefficient of WC-10Co-4Cr increased further at 800 °C. The reason for this behavior is the high oxidation rate at temperatures of 700 °C and higher (Ref 15, 18, 20, 21), illustrated by the micrograph shown in Fig. 8. WC-$(W,Cr)_2C$-Ni coatings showed total wear coefficients of about 10^{-6} mm^3/Nm at temperatures of 800 °C due to a low oxidation rate (see Fig. 9). The total wear rate of 10^{-6} mm^3/Nm characterizes the borderline between dry friction and mixed/boundary lubrication (Ref 18). Therefore, this value characterizes wear couples especially suitable for service under dry sliding conditions. It should also be mentioned that despite the different counterparts, the wear rates found in these experiments are in good agreement with the results described by Ishikawa et al. (Ref 5).

As shown in Fig. 11, the coefficients of friction of WC-10Co-4Cr and WC-$(W,Cr)_2C$-Ni paired with alumina were about 0.5 and higher up to temperatures of 400 °C. Coefficients of friction down to 0.34 were measured at a temperature of 600 °C with increasing sliding speeds. At a test temperature of 800 °C, a coefficient of friction of about 0.4 was measured for WC-$(W,Cr)_2C$-Ni coatings for all sliding speeds.

4. Conclusions

Although the composition of WC-$(W,Cr)_2C$-Ni has been known for about 50 years and commercial powders of this composition are available, only a few investigations have been carried out on it and properties of coatings prepared from it so far.

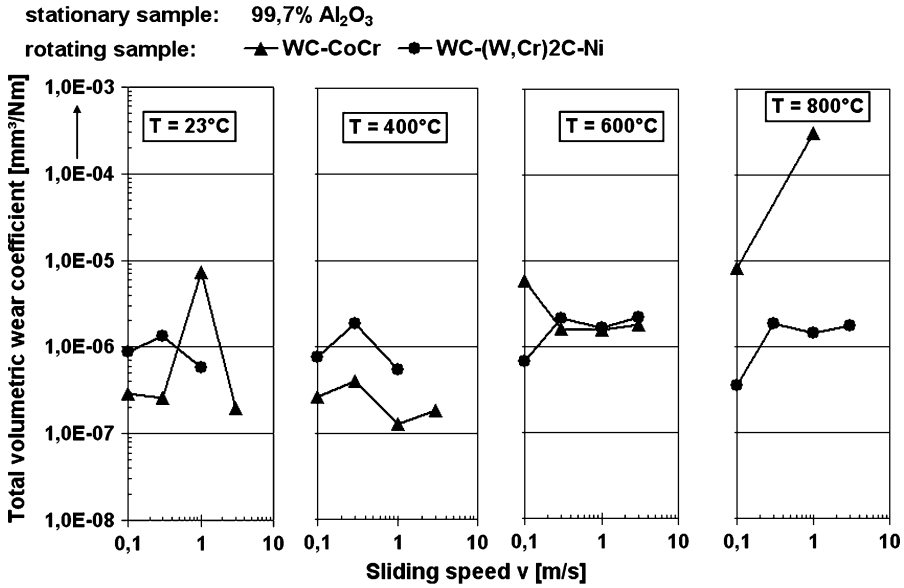

Fig. 10 Total volumetric wear coefficient of WC-CoCr and WC-$(W,Cr)_2C$-Ni coatings tested against sintered alumina (Ref 18, 20)

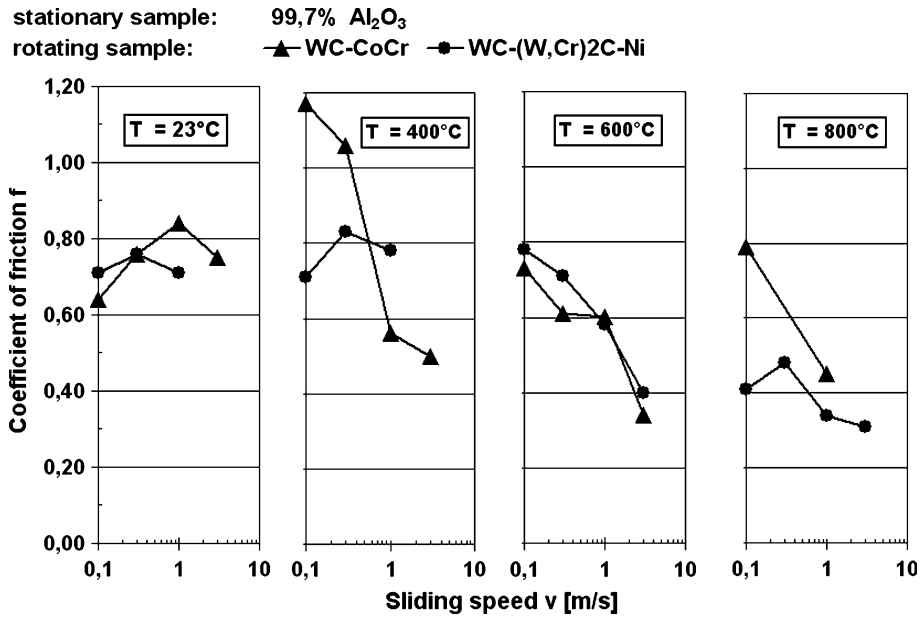

Fig. 11 Dependence of the coefficient of friction on sliding speed and temperature for WC-CoCr and WC-$(W,Cr)_2C$-Ni coatings tested against sintered alumina (Ref 18, 20)

Unlike WC-Co and Cr_3C_2-NiCr, WC-$(W,Cr)_2C$-Ni is not a simple binary hard phase—binder metal composite. The $(W,Cr)_2C$ phase is formed under certain circumstances during feedstock powder preparation. The distribution of $(W,Cr)_2C$ as the second hard phase is often inhomogeneous in the coatings, obviously depending on the method used to produce the feedstock powder. The chromium content of this phase can vary quickly and easily, but information about the changing properties of the phase is missing from the literature. Due to the chromium content, a higher oxygen uptake occurs during spraying compared with spraying of WC-Co and WC-CoCr. It is also surprising that the WC-$(W,Cr)_2C$-7%Ni composition can be sprayed with a high deposition efficiency even though it has a much lower metallic binder content than the other WC-based compositions.

The higher number of crystallographic phases is also responsible for the very complex coating microstructures. Due to the presence of at least two hard phases, the coating properties are not directly dependent on the WC grain size in the coating, unlike for WC-Co coatings.

The properties of WC-$(W,Cr)_2C$-Ni coatings differ significantly from those of other commercially available WC-based standard compositions such as WC-Co and WC-CoCr. In particular, WC-$(W,Cr)_2C$-Ni coatings are characterized by a significantly higher oxidation resistance up to 900 °C. Consequently, this coating can be applied at elevated temperatures. In unlubricated dry sliding wear conditions, the coating is characterized by low wear rates and low coefficients of friction in pairs with alumina. Regarding coating hardness, contradictory data is published in the literature.

The application potential of WC-$(W,Cr)_2C$-Ni coatings has not yet been exhausted. More intensive work is required to answer the open questions on coating phase composition, microstructure, and properties.

Acknowledgments

Ms B. Wolf (Fh-IWS) is thanked for metallographic preparation, Ms A. Richter (Fh-IWS) for SEM, and Dr J. Bretschneider (Fh-IWS) for EDX studies. Ms M. Kašparova's stay at Fh-IWS was supported by the Erasmus program of the European Community.

References

1. J.F. Pelton and J.M. Koffskey Jr., Process of Flame Spraying a Tungsten Carbide-Chromium Carbide-Nickel Coating, and Article Produced Thereby, US Patent 3,071,489 (filing date: 28.05.1958, granted: 01.01.1963)
2. R. Okada and M. Yamada, Effect of Heat Treatment on Hardness and Wear Resistance of WC-NiCr Sprayed Coatings, *J. Jpn. Inst. Met.*, 1994, **58**(7), p 763-767 (in Japanese)
3. Y. Ishikawa, J. Kawakita, S. Osawa, T. Itsukaichi, Y. Sakamoto, M. Takaya, and S. Kuroda, Evaluation of Corrosion and Wear Resistance of Hard Cermet Coatings Sprayed by Using an Improved HVOF Process, *J. Thermal Spray Techn.*, 2005, **14**(3), p 384-390
4. Y. Ishikawa, J. Kawakita, and S. Kuroda, Effect of Spray Condition and Heat Treatment on the Structure and Adhesive Wear Properties of WC Cermet Coatings, *Mater. Trans.*, 2005, **46**(7), p 1671-1676
5. Y. Ishikawa, S. Kuroda, J. Kawakita, Y. Sakamoto, and M. Takaya, Sliding Wear Properties of HVOF Sprayed WC-20%Cr_3C_2-7%Ni Cermet Coatings, *Surf. Coat. Tech.*, 2007, **201**(8), p 4718-4727
6. M. Yoshida, K. Tani, A. Nakahira, A. Nakajima, and T. Mawatari, Durability and Tribological Properties of Thermally Sprayed WC Cermet Coating in Rolling/Sliding Contact, *Thermal Spraying: Current Status and Future Trends*, Vol. 2, A. Ohmori, Ed., May 22-26, Kobe, High Temperature Society of Japan, Japan, 1995, p 663-668
7. A. Nakajima, T. Mawatari, M. Yoshida, K. Tani, and A. Nakahira, Effects of Coating Thickness and Slip Ratio on Durability of Thermally Sprayed WC Cermet Coatings in Rolling/Sliding Contact, *Wear*, 2000, **241**(2), p 166-173
8. D.M. Nuruzzaman, A. Nakajima, and T. Mawatari, Effects of Substrate Surface Finish and Substrate Material on Durability of Thermally Sprayed WC Cermet Coatings in Rolling with Sliding Contact, *Tribol. Int.*, 2006, **39**(7), p 678-685
9. D. Toma, W. Brandl, and G. Marginean, Wear and Corrosion Behaviour of Thermally Sprayed Cermet Coatings, *Surf. Coat. Tech.*, 2001, **138**(2-3), p 149-158
10. H. Henke, D. Adam, A. Köhler, and R.B. Heimann, Development and Testing of HVOF-Sprayed Tungsten Carbide Coatings Applied to Moulds for Concrete Roof Tiles, *Wear*, 2004, **256**(1-2), p 81-87
11. J.E. Cho, S.Y. Hwang, and K.Y. Kim, Corrosion Behaviour of Thermal Sprayed WC Cermet Coatings Having Various Metallic Binders in Strong Acidic Environment, *Surf. Coat. Tech.*, 2006, **200**(8), p 2653-2662
12. H. Kreye, High Velocity Flame Spraying—Process and Coating Characteristics, *Proc. 2nd Plasma-Technik-Symposium*, Vol. 1, S. Blum-Sandmeier, H. Eschnauer, P. Huber, and A.R. Nicoll, Eds., June 5-7, Plasma-Technik AG (Lucerne, Switzerland), 1991, p 39-47
13. P. Stecher, F. Benesovsky, and H. Nowotny, Untersuchungen im System Chrom-Wolfram-Kohlenstoff (Investigations in the System Chromium-Tungsten-Carbon), *Planseeber. Pulvermet.*, 1964, **12**(2), p 89-95 (in German)
14. V.N. Eremenko, T.Y. Velikanova, and A.A. Bondar, The Cr-W-C Phase Diagram at High Temperatures, *Dokl. Akad. Nauk Ukrainskoj SSR, Ser. A, Fiz.-Mat. Nauki* 1986, (11), p 74-78 (in Russian)
15. L.-M. Berger, R. Zieris, and S. Saaro, Oxidation of HVOF-Sprayed Hardmetal Coatings, *Proc. Int. Thermal Spray Conf. ITSC 2005*, May 2-4, DVS-Verlag (Basel, Switzerland), 2005, CD, 8 p
16. S. Zimmermann, H. Keller, and G. Schwier, New Carbide Based Materials for HVOF Spraying, *Thermal Spray 2003: Advancing the Science and Applying the Technology*, Vol. 1, B.R. Marple and C. Moreau, Eds., May 5-8, ASM International (Orlando, FL), 2003, p 227-232
17. J. Beczkowiak, J. Fischer, and G. Schwier, Cermets für das Hochgeschwindigkeits-Flammspritzen (Cermets for HVOF-Spraying), Thermische Spritzkonferenz '93, Vol. 152, Deutscher Verlag für Schweißtechnik, DVS-Berichte, Aachen, Germany, March 3-5, 1993, p 32-36 (in German)
18. L.-M. Berger, S. Saaro, and M. Woydt, Reib-/Gleitverschleiß von thermisch gespritzten Hartmetallschichten (Sliding Wear of Thermally Sprayed Hardmetal Coatings), *Jahrbuch Oberflächentechnik 2007*, Vol. 63, R. Suchentrunk, Ed., Eugen G. Leuze Verlag, 2007, p 242-267 (in German)
19. L.-M. Berger, M. Woydt, S. Zimmermann, H. Keller, G. Schwier, R. Enžl, and S. Thiele, Tribological Behavior of HVOF-Sprayed Cr_3C_2-NiCr and TiC-Based Coatings under High-Temperature Dry Sliding Conditions, *Thermal Spray 2004: Advances in Technology and Application*, May 10-12, ASM International (Osaka, Japan), 2004, p 468-477
20. L.-M. Berger, M. Woydt, and R. Zieris, Comparative Study of HVOF-Sprayed Hardmetal Coatings under High Temperature Dry Sliding Conditions, *Proc. 16th Int. Plansee Seminar, May 30-June 3, 2005*, Vol. 2 (Reutte/Tirol, Austria), G. Kneringer, P. Rödhammer, H. Wildner, Eds., Reutte, Plansee Holding AG, 2005, p 878-892
21. L.-M. Berger, S. Saaro, and M. Woydt, Influence of Oxidation on the Dry Sliding Properties of HVOF-Sprayed Hardmetal Coatings, *Proc. Euro PM2006, Congress & Exhibition, October 23-25, 2006*, Vol. 1 (Ghent, Belgium), Eur. Powder Metallurgy Ass., Shrewsbury, UK, 2006, p 225-232
22. L.-M. Berger, Hardmetals as Thermal Spray Coatings, *Powder Met.*, 2007, **50**(3), p 205-214
23. C. Verdon, A. Karimi, and J.-L. Martin, A Study of High Velocity Oxy-Fuel Thermally Sprayed Tungsten Carbide Based Coatings. Part 1: Microstructures, *Mater. Sci. Eng.*, 1998, **A246**(1-2), p 11-24
24. D.A. Stewart, P.H. Shipway, and D.G. McCartney, Microstructural Evolution in Thermally Sprayed WC-Co Coatings: Comparison between Nanocomposite and Conventional Starting Powders, *Acta Mater.*, 2000, **48**(7), p 1593-1604
25. M. Oechsle, Carbide Containing Spray Powders and HVOF-Coatings, *7. HVOF-Kolloquium 2006*, Gemeinschaft Thermisches Spritzen e.V., Erding, Germany, November 9-10, 2006, p 57-62
26. L.-M. Berger, P. Vuoristo, T. Mäntylä, and W. Gruner, A Study of Oxidation Behaviour of WC-Co, Cr_3C_2-NiCr and TiC-Based Materials in Thermal Spray Processes, *Proc. 15th Int. Thermal Spray Conf. ITSC 1998*, Vol. 1, C. Coddet, Ed., ASM International, Nice, France, May 25-29, 1998, p 75-82
27. L.-M. Berger, M. Woydt, and S. Saaro, Comparison of Self-Mated Hardmetal Coatings under Dry Sliding Conditions up to 600°C, *Wear*, 2008. doi:10.106/j.wear.2008.04.013